

Dalton Transactions

Accepted Manuscript



This is an *Accepted Manuscript*, which has been through the Royal Society of Chemistry peer review process and has been accepted for publication.

Accepted Manuscripts are published online shortly after acceptance, before technical editing, formatting and proof reading. Using this free service, authors can make their results available to the community, in citable form, before we publish the edited article. We will replace this *Accepted Manuscript* with the edited and formatted *Advance Article* as soon as it is available.

You can find more information about *Accepted Manuscripts* in the [Information for Authors](#).

Please note that technical editing may introduce minor changes to the text and/or graphics, which may alter content. The journal's standard [Terms & Conditions](#) and the [Ethical guidelines](#) still apply. In no event shall the Royal Society of Chemistry be held responsible for any errors or omissions in this *Accepted Manuscript* or any consequences arising from the use of any information it contains.

ARTICLE

BSA-directed Synthesis of CuS Nanoparticles as a Biocompatible Photothermal Agent for Tumor Ablation in Vivo

Cite this: DOI: 10.1039/x0xx00000x

Received 00th January 2012,
Accepted 00th January 2012

DOI: 10.1039/x0xx00000x

www.rsc.org/

Cai Zhang,^b Yan-Yan Fu,^a Xuejun Zhang,^a Chunshui Yu,^{ab} Yan Zhao^c and Shao-Kai Sun*^a

Photothermal therapy as a physical therapeutic approach has greatly attracted research interests due to its negligible systemic effects. Among various photothermal agents, CuS nanoparticles have been widely used due to their easy preparation, low cost, high stability and strong absorption in NIR region. However, the ambiguous biotoxicity of CuS nanoparticles limited their bio-application. So it is highly desirable to develop biocompatible CuS photothermal agents with the potential of clinical translation. Herein, we reported a novel method to synthesize biocompatible CuS nanoparticles for photothermal therapy using bovine serum albumin (BSA) as template via mimicking biomaterialization processes. Owing to the inherent biocompatibility of BSA, the toxicity assays in vitro and in vivo showed that BSA-CuS nanoparticles possessed good biocompatibility. In vitro and in vivo photothermal therapies were performed and good results were obtained. Bulk of HeLa cells treated with BSA-CuS nanoparticles under laser irradiation (808 nm) were killed, and the tumor tissues of mice were also successfully eliminated without causing obvious systemic damage. In a word, a novel strategy for synthesis of CuS nanoparticles was developed using BSA as the template, and the excellent biocompatibility and efficient photothermal therapy effects of the BSA-CuS nanoparticles show great potential as an ideal photothermal agent for cancer treatment.

Introduction

Photothermal therapy (PTT) induced by a near-infrared (NIR) laser could kill tumor cells through converting light energy into heat using photothermal agents. Cancer cells are more sensitive to heat than normal cells because of the severely hypoxic and low pH microenvironment.¹ In addition, cancer cells could be selectively ablated by PTT based on three strategies of selectivity, including passive or active tumor homing, intratumoural injection and spatially controlled light illumination. Thus, systemic effects could be minimized in PTT. As a noninvasive approach, photothermal therapy has attracted great research interests.^{2,3}

† Electronic Supplementary Information (ESI) available: materials and methods, characterizations, evaluation of toxicity, PTT in vitro and in vivo. See DOI: 10.1039/x0xx00000x

To date, various attractive nanomaterials with strong NIR absorption, such as organic dyes,⁴⁻⁶ noble metal materials,⁷ carbon-based nanostructures,^{8,9} semiconductor compounds¹⁰⁻¹⁵ and polymers^{16,17} have been used as photothermal agents for PTT. Particularly, copper sulfide nanomaterials have attracted widespread attention because of their low toxicity, easy preparation, low cost and high stability.¹⁸⁻³¹ Additionally, the NIR absorption of CuS nanoparticles is derived from d-d transition of Cu²⁺ ions, which makes the CuS nanoparticles own the ability of resisting the change of the surrounding environment and long-term light irradiation. Thus, CuS nanoparticles are increasingly employed in photothermal ablation. The biosafety of CuS nanoparticles plays a crucial role in biological application.^{30,32} Currently, several ligands, such as thioglycolic acid,¹⁸ sodium citrate,^{19,25,31} polyvinyl pyrrolidone,^{20,27,33,34} sodium dodecyl sulfate,²³ gelatin,²⁴ thiol-polyethylene glycol,²⁶ chitosan²⁸ and cysteine,²⁹ have been employed to synthesize CuS nanoparticles with NIR absorption. However, the ambiguous biotoxicity and limited systemic toxicity evaluation of CuS nanoparticles hindered their bio-application towards clinical

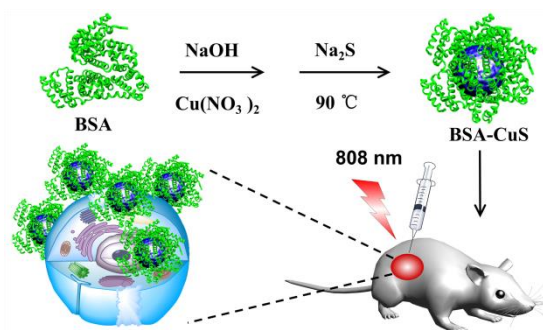
^aSchool of Medical Imaging, Tianjin Medical University, Tianjin 300203, China

Email: shaokaisun@163.com

^bDepartment of Radiology, Tianjin Key Laboratory of Functional Imaging, Tianjin Medical University General Hospital, Tianjin 300052, China.

^cTianjin Institute of infectious diseases, the Second Hospital of Tianjin Medical University, Tianjin 300211, China

translation, and few reports focused on this.³⁴ So it is highly desired to develop novel CuS-based photothermal agents with excellent biocompatibility.



Scheme 1. Schematic Illustration of the Fabrication of BSA-CuS Nanoparticles as a Photothermal Agent for Tumor Ablation

Recently, an encouraging way to fabricate biocompatible nanomaterials using biomacromolecules as stabilized agents was developed via mimicking biomaterialization processes,³⁵ which benefits from biosafety, high efficiency and mild synthesis condition. Typically, albumin is widely selected as a biocompatible template for the synthesis of nanoparticles due to its abundant functional groups, such as thiol, amine, and carboxyl groups. Au,³⁶ Ag,³⁷ ZnS/Mn,³⁸ HgS,³⁹ Gd₂O₃/Gd(OH)₃⁴⁰ and Gd₂O₃/Au⁴¹ nanostructures stabilized by albumin have been studied extensively. More important, albumin has been used as a viable drug carrier for administering chemotherapeutic drugs, which has been approved by U.S. Food and Drug Administration (FDA) for the treatment of several cancers in clinic.⁴² So it is very attractive to develop albumin-directed CuS photothermal agents with excellent inherent biocompatibility.

Herein, we reported a simple synthetic route to construct biocompatible albumin-directed CuS photothermal agents with excellent inherent biocompatibility for cancer treatment (Scheme 1). Systemic evaluation of the cytotoxicity and toxicity in vivo demonstrated the good biocompatibility of the proposed BSA-CuS nanoparticles. Photothermal therapies in vitro and in vivo were performed. Bulk of the tumor cells in vitro treated with BSA-CuS under 808 nm laser irradiation were destructed, and the tumor tissues in vivo were also successfully eliminated without causing obvious systemic damage.

Experimental

Chemicals

All chemicals and reagents used were at least of analytical grade. Ultrapure water (Hangzhou Wahaha Group Co. Ltd., Hangzhou, China) was used throughout this work. BSA was obtained from Beijing Dingguo Biotechnology Co., Ltd. (Beijing, China). Cu(NO₃)₂·3H₂O, Na₂S·9H₂O, CaCl₂, trypsin and 3-(4,5-Dimethylthiazol-2-yl)-2,5-diphenyltetrazolium bromide (MTT) were purchased from Aladdin Reagent Co. Ltd. (Shanghai, China). NaOH was bought from Guangfu Fine Chemical Research Institute (Tianjin, China). DMSO were provided from Concord Technology (Tianjin, China)

Characterization

The X-ray diffraction (XRD) analysis was performed on a D/max-2500 diffractometer (Rigaku, Japan). X-ray photoelectron spectroscopy (XPS) measurements were performed on an Axis Ultra

DLD spectrometer fitted with a monochromated Al K α X-ray source ($h\nu = 1486.6$ eV), hybrid (magnetic/electrostatic) optics, and a multichannel plate and delay line detector (Kratos Analytical, Manchester, UK). The morphology and microstructure of BSA-CuS nanoparticles were characterized by a Philips Tecnai G² F20 (Philips, Holland) field emission high-resolution transmission electron microscopy (HRTEM). The samples for HRTEM were prepared by depositing with a dilute nanoparticles solution into a 230-mesh Cu grid, sample droplets dried from water dispersion. The Fourier transform infrared (FT-IR) spectra (400-4000 cm⁻¹) were measured with a Nicolet IR AVATAR-360 spectrometer (Nicolet, USA) with pure KBr as the background. UV-vis absorption spectra were recorded using a UV-3600 UV-Vis-NIR spectrophotometer (Shimadzu, Japan). Dynamic light scattering (DLS) and zeta potential were carried out on a Malvern Zetasizer (Nano series ZS, UK). BSA-CuS nanoparticles in PBS solution were filtrated through 220 nm film before the measurements of DLS and zeta potential.

Synthesis

The BSA-CuS nanoparticles were prepared via a facile method. In a typical procedure, 250 mg of BSA was dissolved in 7.5 mL ultrapure water and 1 mL of 0.2 M of Cu(NO₃)₂ was added to the above solution under magnetic stirring, resulting in a blue mixture. After quickly adding 0.5 mL of 1 M NaOH, the mixture turned to purple. Then 2 mL of 0.2 M Na₂S was added, and the color of the solution turned to brick red at once. The solution was further proceeded at 90 °C for 0.5 h, and the color turned to dark green, which indicated the formation of BSA-CuS nanoparticles. The obtained BSA-CuS nanoparticles were purified for 24 h by dialysis (Mw 8k Da), then freeze-dried and stored at 4 °C for later use. The BSA-CuS nanoparticles used in the following experiments were dissolved in PBS solution and filtrated through 220 nm film.

Colloidal Stability

The stability of BSA-CuS nanoparticles were investigated through incubating different concentrations of BSA-CuS nanoparticles with pure water, PBS (pH = 7.4), normal saline (0.9%) and serum.

Measurement of Photothermal Performance

The solutions of BSA-CuS nanoparticles with different concentrations (192, 640, 1280 mg/L) were irradiated with a laser (808 nm) at a power density of 3.0 W/cm² for 10 min to evaluate the photothermal performance. A thermocouple probe was inserted into solution of BSA-CuS nanoparticles to record the temperature change.

Cell Cultures

Hela cells (human cervical carcinoma cell) were cultured in RPMI-1640 medium (GIBCO) which supplemented with 10% fetal bovine serum and 1% penicillin-streptomycin at 37 °C under a humidified atmosphere with 5% CO₂. Cells were resuspended in fresh complete medium before plating.

Cytotoxicity of BSA-CuS Nanoparticles

Cytotoxicity was measured using the MTT assay in Hela cells. Hela cells were seeded into a 96-well plate (10⁴ cells per well) and incubated for 24 h at 37 °C under 5% CO₂. Then, Hela cells were incubated with various concentrations of BSA-CuS nanoparticles for 24 h. After washing with PBS and treating with MTT (10 μ L, 5 mg/mL) for 4 h, 120 μ L DMSO were added into the cells and the absorbance of the solution in each well was recorded by a multi-mode microplate reader. Six replicates were prepared for each treatment group.

In Vitro Photothermal Therapy of BSA-CuS Nanoparticles

Hela cells were incubated in a 96-well culture plate (10⁴ cell per well) for 24 h at 37 °C under 5% CO₂ and washed with PBS. Then

the cells were treated with BSA-CuS nanoparticles (192 mg/L) for 30 min at 37 °C and exposed to 808 nm laser with power densities of 5.3 and 8.3 W/cm² for 5 or 10 min. Cell viability was evaluated following by the photothermal therapy through MTT assays and inverted luminescence microscope. Calcein AM (calcein acetoxymethyl ester) and PI (propidium iodide) were used to stain live and dead cells, then the luminescence images were acquired.

In Vivo Photothermal Therapy of BSA-CuS Nanoparticles

Hela cells were suspended in RPMI-1640 medium (2×10⁶ cell/100 μL) and inoculated subcutaneously into bilateral inguinal region of Balb/c nude mice (22-24 g, Beijing HFK Bioscience Co. Ltd., Beijing, China). All the operations of animal experiments were approved by the Tianjin Medical University Animal Care and Use Committee. The mice were used for PTT assay after the tumor size grew up to 7-10 mm. The tumor on one side of the mice was irradiated with a 808 nm laser at a power density of 0.7 W/cm² for 15 min after injection with 100 μL of PBS or BSA-CuS solutions (3.84 mg/mL) intratumorally. The tumor on the other side was used as control without any treatment. The tumor photos were taken every day.

In Vivo Toxicity

Kunming mice (29-31 g, Beijing HFK Bioscience Co. Ltd., Beijing, China) were used to evaluate the in vivo toxicity of BSA-CuS nanoparticles. Comprehensive blood biochemical analysis, especially the biomarkers associated with the functions of liver and kidney were performed on mice at 24 h and 7 days after subcutaneously injecting 100 μL of BSA-CuS solutions (3.84 mg/mL). The weight of the mice treated with BSA-CuS (100 μL 3.84 mg/mL) and PBS were also monitored.

Results and discussion

Synthesis and Characterization of BSA-CuS Nanoparticles

BSA was chosen as a model template due to its commercial availability, low cost and good biocompatibility. As the most affluent blood protein, BSA contains 35 potential thiol groups including 17 disulfide bonds and 1 free cysteine, which could be used to stabilize CuS nanoparticles due to the strong affinity between Cu and thiol groups. As shown in Figure 1, before the addition of NaOH, the BSA-Cu²⁺ mixture appeared cloudy and opaque, which indicated the coordination interaction between Cu²⁺ and functional groups including amine, carboxyl and thiol groups in BSA. Alkaline environment could promote BSA to unfold tertiary configuration and expose more available amine acid, and the result loose structures are much efficient in the control of the crystal growth and encapsulation of CuS nanoparticles. Therefore, the mixture with a low concentration of Cu²⁺ was transparent upon addition of NaOH, while the mixture with a high concentration of Cu²⁺ remained cloudy due to the limited encapsulation ability of the unfolded BSA. After the addition of Na₂S, the mixture changed to brown at once, which indicated the formation of CuS nanoparticles.

The size of BSA-CuS nanoparticles was characterized by HRTEM, and the nanoparticles show a size of 14 nm (Figure 2a). The hydrodynamic size of the nanoparticles was measured by dynamic light scattering, and the result was about 60 nm, which was an appropriate size for the application in vivo. The zeta potential was -21.2 mV, due to the presence of carboxyl groups in BSA, which ensured the aqueous solubility and stability of the nanoparticles. As shown in FT-IR spectra in Figure 2b, the pure BSA showed the characteristic bands for -OH at 3282 cm⁻¹, amide I at 1644 cm⁻¹, and amide II bands at 1532 cm⁻¹, respectively. All the characteristic bands could be found in BSA-CuS nanoparticles, which indicated

the presence of BSA in the prepared BSA-CuS nanoparticles. The phase structure of BSA-CuS nanoparticles was determined by XRD. As shown in Figure S1, all recorded peaks can be assigned to the hexagonal phase of CuS (JCPDS No. 06-0464). To investigate the species of Cu in the synthesized nanoparticles, XPS analysis was

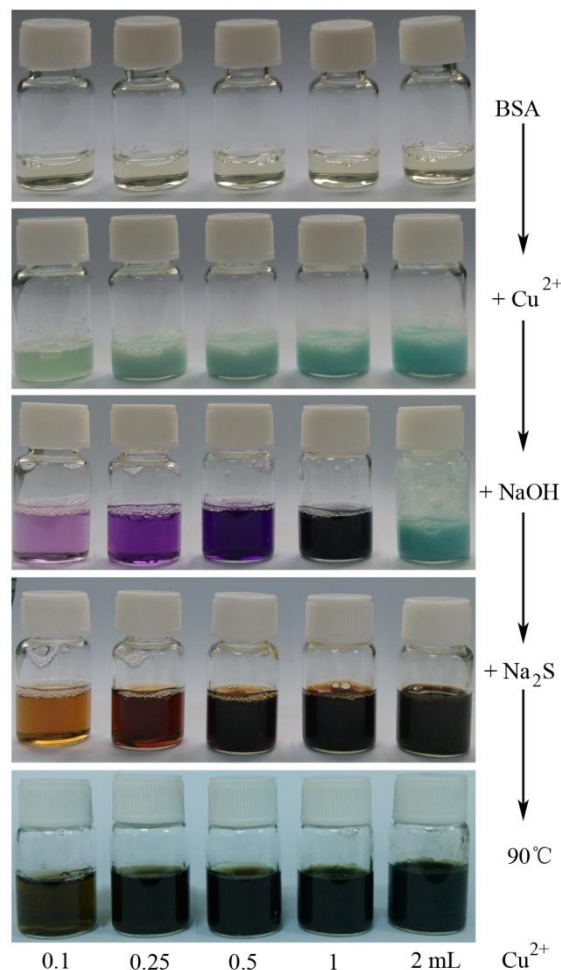


Figure 1. Color changes at different stages in synthesis of BSA-CuS nanoparticles with different dosages of Cu(NO₃)₂ (0.1 mL, 0.25 mL, 0.5 mL, 1 mL, 2 mL) under the condition of fixed molar ratio of S to Cu (2:1).

performed. As shown in Figure S2, XPS peaks at 933.5 eV and 953.6 eV are assigned to Cu 2p_{3/2} and Cu 2p_{1/2} respectively, which in agreement with the literatures.^{27, 43-45} Furthermore, the shake-up satellites, located at 941.3 eV and 963.0 eV respectively, are typical of the Cu²⁺ (3d⁹) species, which further confirmed higher oxidation state of copper as Cu²⁺.^{27, 43-45}

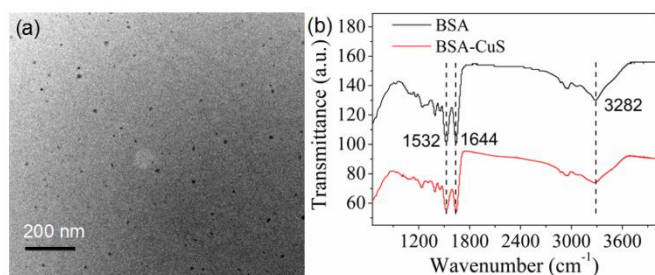


Figure 2. (a) HRTEM image of BSA-CuS nanoparticles. (b) FT-IR spectra of BSA and BSA-CuS nanoparticles.

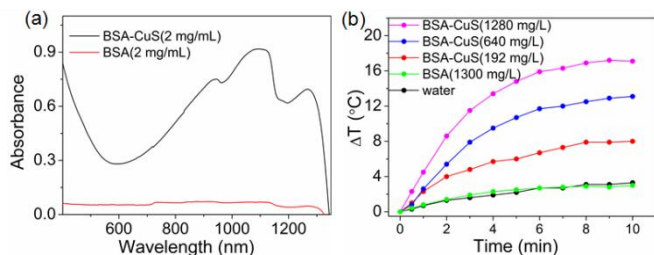


Figure 3. (a) UV-vis-NIR absorption spectra of the BSA-CuS nanoparticles and pure BSA solution. (b) The photothermal heating curves of pure water, pure BSA solution and BSA-CuS nanoparticles dissolved in PBS buffer with different concentrations irradiated by a 808 nm laser irradiation at the power density of 3.0 W/cm².

In order to obtain the maximum NIR absorption of the BSA-CuS nanoparticles with fixed concentration of BSA, the dosage of Cu(NO₃)₂ and the molar ratio of S to Cu were systemically investigated. As shown in Figure S3a, the BSA-CuS nanoparticles showed the biggest absorbance in NIR region when the ratio of S to Cu is 2:1. Subsequently, the dosage of Cu(NO₃)₂ was optimized with S:Cu fixed to 2:1 (Figure S4). It had been found that the absorbance of the BSA-CuS nanoparticles increased as the volume of Cu(NO₃)₂ increased from 0.1 mL to 1 mL (Figure S3b). It could be found the maximum absorption wavelength of the nanoparticles was almost independent on the size of nanoparticles as the absorption of CuS nanoparticles were derived from the d-d transition of Cu²⁺ ion (Figure S5). When the dosage of Cu(NO₃)₂ reached to more than 1 mL, excess CuS could not be entrapped by BSA, leading to the emergence of precipitation. It should be noted that, compared with reaction in room temperature, heating at 90 °C played a crucial role in the preparation of BSA-CuS nanoparticles with stronger NIR absorbance (Figure S3c). The results indicate that the absorption in NIR region of samples highly depends on the ratio of S to Cu, concentration of Cu(NO₃)₂ and the reaction temperature. Optimal experimental conditions for BSA-CuS nanoparticles were obtained. Namely, 250 mg of BSA was dissolved in 7.5 mL ultrapure water and 1 mL of 0.2 M of Cu(NO₃)₂ was added to the above solution under constant stirring. After quickly added 0.5 mL of 1 M NaOH, then 2 mL of 0.2 M Na₂S was added. The solution was further proceeded at 90 °C for 0.5 h, then the BSA-CuS nanoparticles were obtained. The proposed BSA-CuS nanoparticles showed strong absorption in the region of 700-1200 nm (Figure 3a), while BSA alone showed neglectable absorption in NIR region. There was a good linear correlation between the absorbance at 808 nm and the

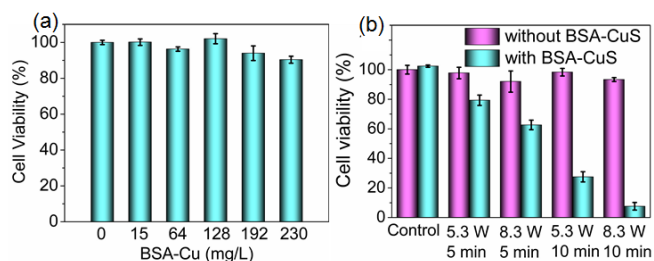


Figure 4. (a) Viability of HeLa cells before and after treated with different concentrations of BSA-CuS nanoparticles. (b) Relative viability of HeLa cells treated with or without BSA-CuS nanoparticles (192 mg/L) under 808 nm laser irradiation with different times and power density; HeLa cells treated with or without BSA-CuS nanoparticles were regarded as control groups.

concentrations of BSA-CuS nanoparticles (Figure S3d). As shown in Figure S6, there were no precipitations appeared in BSA-CuS solution after incubating different concentrations of BSA-CuS nanoparticles with pure water, PBS, normal saline, serum for 12 days. The results demonstrated that BSA-CuS nanoparticles own good colloidal stability due to the efficient protection of BSA.

Measurement of Photothermal Performance

The strong NIR absorption of BSA-CuS nanoparticles motivated us to investigate their photothermal capability. The photothermal effects of BSA-CuS nanoparticles in PBS with different concentrations were evaluated by laser (808 nm) irradiation with a power density of 3.0 W/cm² for 10 min. As shown in Figure 3b, the temperatures of the solution of BSA-CuS nanoparticles with different concentrations increased from 8 to 17.1 °C in 10 min, while the temperature of pure water and BSA solution were only raised by 3.3 and 3 °C respectively under the same condition. The above results demonstrated the prepared BSA-CuS nanoparticles could efficiently converted laser energy to heat via strongly absorbing the NIR light, which could be further used for in vitro and in vivo PTT.

Cytotoxicity of BSA-CuS Nanoparticles

To evaluate the cytotoxicity of BSA-CuS nanoparticles, HeLa cells were incubated with different concentrations of BSA-CuS nanoparticles for 24 h, and a standard MTT assay was carried out to determinate the cell viability. As shown in Figure 4a, high cell viability (>92%) could be obtained with concentration as high as 230 mg/L of BSA-CuS nanoparticles, indicating low cytotoxicity of the prepared photothermal agents, which was probably benefit from

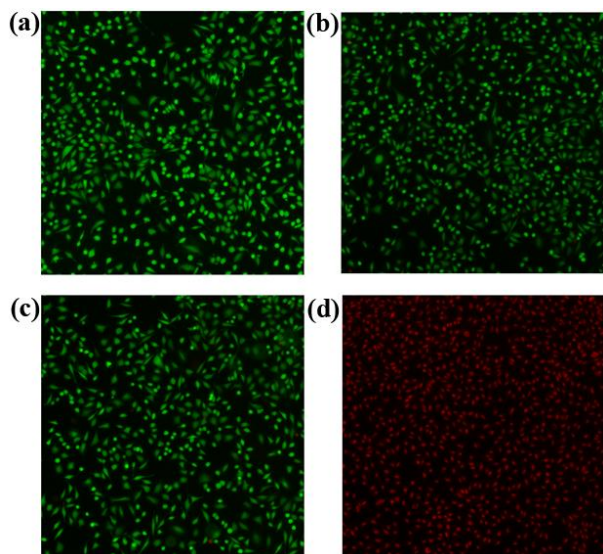


Figure 5. HeLa cells with different treatments were stained with calcein AM and PI, and live and dead cells were stained to be green and red, respectively. (a) HeLa cells without any treatment; (b) HeLa cells incubated with BSA-CuS nanoparticles (192 mg/L); (c) HeLa cells treated with 808 nm laser irradiation (8.3 W/cm^2) for 10 min; (d) HeLa cells treated with BSA-CuS nanoparticles (192 mg/L) under 808 nm laser irradiation (8.3 W/cm^2) for 10 min.

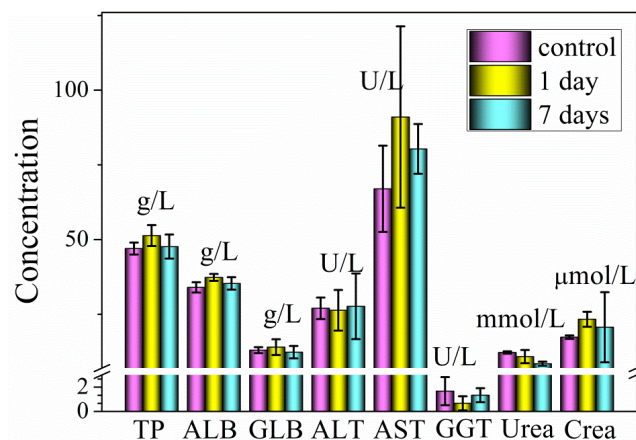


Figure 6. The blood level of TP, ALB, GLB, ALT, AST, GGT, Urea and Crea from the mice at different time points treated with and without BSA-CuS nanoparticles ($100 \mu\text{L}$, 3.84 mg/mL).

biocompatible BSA as the stabilizing template. It should be noted that the proposed nanoparticles showed a similar cytotoxicity with PVP-CuS nanoplates, and both of them showed neglectable cytotoxicity when the concentration was below 200 mg/L .³⁴

In Vitro Photothermal Therapy of BSA-CuS Nanoparticles

The efficient photothermal effect and low cytotoxicity of BSA-CuS nanoparticles encouraged us to investigate the photothermal therapeutic capability in vitro, which was evaluated on HeLa cells through MTT assays and inverted luminescence microscope. HeLa cells were treated without or with different concentrations of BSA-CuS nanoparticles for 30 min at 37°C and exposed to 808 nm laser

with power densities of 5.3 W or 8.3 W/cm^2 for 5 or 10 min. As shown in Figure 4b and 5, the in vitro cytotoxicity MTT assay results showed there were no obvious changes of HeLa cells viability with or without BSA-CuS nanoparticles. Furthermore, exposure of the HeLa cells to laser irradiation alone also remained approximately 93% of cell viability even at a density of 8.3 W/cm^2 for 10 min (Figure 4b). However, HeLa cells treated with BSA-CuS nanoparticles under laser irradiation resulted in a significant cell destruction, especially when the irradiation density and time increased. Approximately, less than 8% cells survived when the cells were irradiated by a 8.3 W/cm^2 NIR laser for 10 min. These results demonstrated that the BSA-CuS nanoparticles have a good photothermal effect on tumor cells.

In vivo toxicity

To evaluate in vivo toxicity of the prepared BSA-CuS nanoparticles, blood biochemical analysis and body weight monitoring were performed. In blood biochemical analysis, the liver function markers including total protein (TP), serum albumin (ALB), globulin (GLB), alanine aminotransferase (ALT), aspartate aminotransferase (AST) and gamma glutamyl transferase (GGT), kidney function markers including urea (Urea) and creatinine (Crea) were all measured at different time points after injection of BSA-CuS ($100 \mu\text{L}$, 3.84 mg/mL). As shown in Figure 6, all the parameters in the experimental groups were found to be normal compared with those

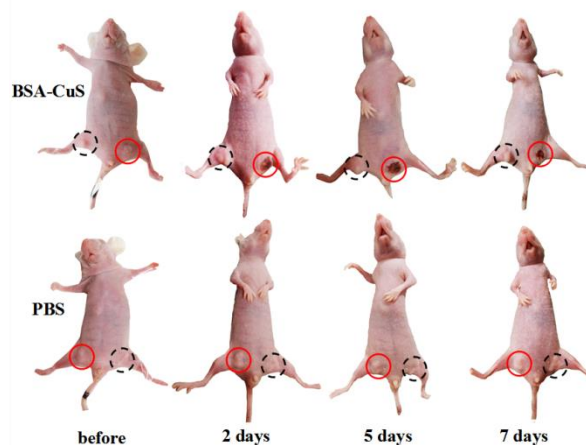


Figure 7. Representative photos of mice bearing tumors at different time points post-injection of BSA-CuS nanoparticles or PBS (solid line circles) under 808 nm laser irradiation; The tumors without any treatment were regarded as the intraindividual control groups (dotted circles).

in the control group, illustrating no obvious hepatic damage and kidney disorder induced by BSA-CuS nanoparticles (3.84 mg/mL) at a dose of $100 \mu\text{L}$. Furthermore, there was no obvious difference in body weight between the mice treated with BSA-CuS nanoparticles and the control group within 10 days (Figure S7). These results indicated the BSA-CuS nanoparticles have low toxicity and negligible side effect, and could be used for in vivo PTT.

In vivo Photothermal Therapy of BSA-CuS Nanoparticles
Encouraged by the efficient photothermal ability of BSA-CuS nanoparticles and biosafety in vitro and in vivo, Hela cells bearing nude mice were selected to further evaluate the antitumor effect of BSA-CuS nanoparticles. The tumor on one side of the mice was intratumorally injected with 100 μ L of PBS or BSA-CuS nanoparticles before irradiated under 0.7 W/cm² NIR laser light (808 nm) for 15 min, while the tumor on the other side were kept without any treatment. The tumor photos were taken every day to monitor weight changes of the tumor at different time points (Figure S8). It can be seen from Figure 7, the tumors treated with PBS (solid line circles) and without any treatment (dotted circles) continued to grow rapidly, while the tumor treated with BSA-CuS nanoparticles under laser irradiation were significantly inhibited and dispelled completely at last. These results clearly demonstrated that the BSA-CuS nanoparticles could be used as a superior photothermal probe with good biocompatibility for PTT of tumors in vivo.

Conclusions

In conclusion, we have reported a novel strategy to synthesis biocompatible CuS nanoparticles for in vivo PTT using BSA as template due to its commercial availability, low cost and good biocompatibility. More important, the protein-directed synthesis own the advantages in the aspects of excellent colloidal and good biocompatibility since it is an inherent biomacromolecule in living organisms. The low cytotoxicity and negligible toxicity in vivo were proved by MTT assays and blood biochemical analysis, weight monitoring. The tumor cells treated with the nanoparticles under irradiation were effectively damaged. Furthermore, the tumor of the mice treated with BSA-CuS nanoparticles were eliminated by laser irradiation with low power density in a short irradiation time without causing obvious systemic damage. Owing to the excellent good therapy effect and low toxicity both in vitro and in vivo, BSA-CuS nanoparticles show great potential as a promising PTT agent for further photothermal biological applications.

Acknowledgements

This work was supported by the National Natural Science Foundation of China (Grants 21405112, 21435001), China Postdoctoral Science Foundation (Grants 2014M550146).

References

1. J. van der Zee, *Ann Oncol*, 2002, **13**, 1173-1184.
2. L. Cheng, C. Wang, L. Feng, K. Yang and Z. Liu, *Chem Rev*, 2014, **114**, 10869-10939.
3. E.-K. Lim, T. Kim, S. Paik, S. Haam, Y.-M. Huh and K. Lee, *Chem Rev*, 2015, **115**, 327-394.
4. Y. Caixia, L. Peng, Z. Mingbin, Z. Pengfei, W. Yiqing, M. Yifan and C. Lintao, *Biomaterials*, 2013, **34**, 6853-6861.
5. Q. Chen, C. Wang, Z. Zhan, W. He, Z. Cheng, Y. Li and Z. Liu, *Biomaterials*, 2014, **35**, 8206-8214.
6. P. Huang, P. Rong, A. Jin, X. Yan, M. G. Zhang, J. Lin, H. Hu, Z. Wang, X. Yue, W. Li, G. Niu, W. Zeng, W. Wang, K. Zhou and X. Chen, *Adv Mater*, 2014, **26**, 6401-6408.
7. A. J. Mieszawska, W. J. M. Mulder, Z. A. Fayad and D. P. Cormode, *Molecular Pharmaceutics*, 2013, **10**, 831-847.
8. Z. Liu and X. J. Liang, *Theranostics*, 2012, **2**, 235-237.
9. K. Yang, L. Z. Feng, X. Z. Shi and Z. Liu, *Chem Soc Rev*, 2013, **42**, 530-547.
10. Z. Chen, Q. Wang, H. Wang, L. Zhang, G. Song, L. Song, J. Hu, H. Wang, J. Liu, M. Zhu and D. Zhao, *Adv Mater*, 2013, **25**, 2095-2100.
11. S. S. Chou, B. Kaehr, J. Kim, B. M. Foley, M. De, P. E. Hopkins, J. Huang, C. J. Brinker and V. P. Dravid, *Angew Chem Int Ed*, 2013, **52**, 4160-4164.
12. L. Cheng, J. Liu, X. Gu, H. Gong, X. Shi, T. Liu, C. Wang, X. Wang, G. Liu, H. Xing, W. Bu, B. Sun and Z. Liu, *Adv Mater*, 2014, **26**, 1886-1893.
13. S. Goel, F. Chen and W. Cai, *Small*, 2014, **10**, 631-645.
14. W. Yin, L. Yan, J. Yu, G. Tian, L. Zhou, X. Zheng, X. Zhang, Y. Yong, J. Li, Z. Gu and Y. Zhao, *Acs Nano*, 2014, **8**, 6922-6933.
15. S. Wang, K. Li, Y. Chen, H. Chen, M. Ma, J. Feng, Q. Zhao and J. Shi, *Biomaterials*, 2015, **39**, 206-217.
16. Z. Zha, X. Yue, Q. Ren and Z. Dai, *Adv Mater*, 2013, **25**, 777-782.
17. L. Xu, L. Cheng, C. Wang, R. Peng and Z. Liu, *Polymer Chemistry*, 2014, **5**, 1573-1580.
18. Y. B. Li, W. Lu, Q. A. Huang, M. A. Huang, C. Li and W. Chen, *Nanomedicine*, 2010, **5**, 1161-1171.
19. M. Zhou, R. Zhang, M. Huang, W. Lu, S. Song, M. P. Melancon, M. Tian, D. Liang and C. Li, *J Am Chem Soc*, 2010, **132**, 15351-15358.
20. Q. W. Tian, M. H. Tang, Y. G. Sun, R. J. Zou, Z. G. Chen, M. F. Zhu, S. P. Yang, J. L. Wang, J. H. Wang and J. Q. Hu, *Adv Mater*, 2011, **23**, 3542-3547.
21. S. Goel, F. Chen and W. Cai, *Small*, 2013, **10**, 631-645.
22. G. Song, Q. Wang, Y. Wang, G. Lv, C. Li, R. Zou, Z. Chen, Z. Qin, K. Huo, R. Hu and J. Hu, *Adv Funct Mater*, 2013, **23**, 4281-4292.
23. Y. Wang, Y. Xiao, H. Zhou, W. Chen and R. Tang, *Rsc Advances*, 2013, **3**, 23133-23138.
24. Z. Zha, S. Zhang, Z. Deng, Y. Li, C. Li and Z. Dai, *Chem Commun*, 2013, **49**, 3455-3457.
25. Z. B. Zha, S. M. Wang, S. H. Zhang, E. Z. Qu, H. T. Ke, J. R. Wang and Z. F. Dai, *Nanoscale*, 2013, **5**, 3216-3219.
26. S. Zhang, Z. Zha, X. Yue, X. Liang and Z. Dai, *Chem Commun*, 2013, **49**, 6776-6778.
27. X. Bu, D. Zhou, J. Li, X. Zhang, K. Zhang, H. Zhang and B. Yang, *Langmuir*, 2014, **30**, 1416-1423.
28. L. Guo, D. D. Yan, D. Yang, Y. Li, X. Wang, O. Zalewski, B. Yan and W. Lu, *Acs Nano*, 2014, **8**, 5670-5681.
29. X. Liu, B. Li, F. Fu, K. Xu, R. Zou, Q. Wang, B. Zhang, Z. Chen and J. Hu, *Dalton Trans*, 2014, **43**, 11709-11715.
30. Z. Xiao, *Nanomedicine*, 2014, **9**, 373-375.
31. K. Yang, L. Zhu, L. Nie, X. Sun, L. Cheng, C. Wu, G. Niu, X. Chen and Z. Liu, *Theranostics*, 2014, **4**, 134-141.
32. S. Sharifi, S. Behzadi, S. Laurent, M. L. Forrest, P. Stroeve and M. Mahmoudi, *Chem Soc Rev*, 2012, **41**, 2323-2343.
33. S. Ramadan, L. R. Guo, Y. J. Li, B. F. Yan and W. Lu, *Small*, 2012, **8**, 3143-3150.
34. W. Feng, W. Nie, Y. Cheng, X. Zhou, L. Chen, K. Qiu, Z. Chen, M. Zhu and C. He, *Nanomedicine*, 2015, **11**, 901-912.

Journal Name

35. N. Ma, A. F. Marshall and J. H. Rao, *J Am Chem Soc*, 2010, **132**, 6884–6885.
36. J. P. Xie, Y. G. Zheng and J. Y. Ying, *J Am Chem Soc*, 2009, **131**, 888–889.
37. C. L. Guo and J. Irudayaraj, *Anal Chem*, 2011, **83**, 2883–2889.
38. P. Wu, T. Zhao, Y. Tian, L. Wu and X. Hou, *Chem Eur J*, 2013, **19**, 7473–7479.
39. N. Goswami, A. Giri, S. Kar, M. S. Bootharaju, R. John, P. L. Xavier, T. Pradeep and S. K. Pal, *Small*, 2012, **8**, 3175–3184.
40. B. Zhang, H. Jin, Y. Li, B. Chen, S. Liu and D. Shi, *J Mater Chem*, 2012, **22**, 14494–14501.
41. S.-K. Sun, L.-X. Dong, Y. Cao, H.-R. Sun and X.-P. Yan, *Anal Chem*, 2013, **85**, 8436–8441.
42. F. Kratz, *J. Control. Release*, 2014, **190**, 331–336.
43. J. F. Moulder, W. F. Stickle, P. E. Sobol and K. Bomben, *Handbook of X-Ray Photoelectron Spectroscopy, 2nd edn, Peikin-Elmer Corporation (Physical Electronics), USA, 1992*.
44. L. Armelao, D. Camozzo, S. Gross and E. Tondello, *J. Nanosci. Nanotechnol.*, 2006, **6**, 401–408.
45. V. Krylova and A. Andrulevicius, *Int. J. Photoenergy*, 2009, **2009**, 304308.